Available online at www.sciencedirect.com
SCIENCE DIRECT
Journal of Power Sources 156 (2006) 725–740
JOURNAL OF POWER SOURCES
www.elsevier.com/locate/jpowsour

Requirements for performance characterization of C double-layer supercapacitors: Applications to a high specific-area C-cloth material

Jianjun Niu, Wendy G. Pell, Brian E. Conway *

Department of Chemistry, University of Ottawa, 10 Marie Curie Street, Ottawa, Ont., Canada K1N 6N5

Received 20 April 2005; received in revised form 31 May 2005; accepted 1 June 2005
Available online 22 July 2005

Abstract

Electrochemical capacitors, based on the double-layer capacitance of high specific-area C materials, are attracting major fundamental and technological interest as highly reversible, electrical charge-storage and delivery devices, capable of being operated at high power-densities. A variety of applications have been described in the literature, e.g. for cold-start vehicle assist, in hybrid load-leveling configurations with batteries, fuel-cells, as well as directly with internal combustion engines. Additionally, high capacitance C electrodes have been usefully employed as anodes coupled with battery-type cathodes, e.g. Pb/PbO_2, in so-called "asymmetric" capacitor cells.

On account of these perceived various applications, requirements for performance evaluation must be developed in systematic and complementary ways. In the present paper, we examine experimentally the following test procedures as exemplified by application to an high specific-area (ca. $2500\,m^2\,g^{-1}$) woven C-cloth capacitor electrode material: (i) evaluation of the specific capacitances as a function of charge/discharge rates employing cyclic-voltammetry and dc charging curves; (ii) as in (i), examination of reversibility and energy-efficiency as a function of electrolyte (H_2SO_4) concentration, i.e. conductivity; (iii) interpretation of effects in (i) and (ii) in terms of distributed resistance and capacitance in the porous C matrix according to the de Levie model; (iv) interpretation of data obtained in (i) in terms of Ragone plots which, for capacitor devices, require special treatment owing to the fundamental dependence of electrode- (or device) potential on state of discharge; (v) interpretation of self-discharge (SD) kinetics in terms of porous-electrode structure. Performance data for the C-electrode are given for capacitative charging up to high "C-rates", extension of operational voltage windows and for SD behaviour.

Keywords: Electrochemical capacitors; Supercapacitors; Carbon cloth electrode; Self-discharge; Float-current

1. Introduction

In recent years, research and development of electrochemical capacitors (ECs) has become a challenging and technologically important field [1–5] due to their perceived high operating power-density and to demands for new applications involving high specific-power sources for power trains of electric vehicles that can be operated with less or zero toxic gas emission. However, compared with batteries, an EC usually provides lower energy-density and exhibits higher self-discharge rates which make it impossible to be simply a substitute for batteries in commercial or industrial applications. Additionally, the approximately linear decline of voltage with declining state-of-charge (SOC) is a fundamental aspect of a capacitor's electrical behaviour. However, opportunities arise for *complementary operation* of ECs that are electrically coupled in discharge and recharge with batteries to obtain more efficient charge storage and power delivery. Special attention has been recently given to the development of hybrid battery–capacitor systems for electric-vehicle drive trains [6–9]. Also, testing results have been reported for hybrid power sources based on a combination of capacitor and battery-type electrodes [6,10] and a projected EC with an energy-density of $20\,kJ\,kg^{-1}$ and a power-density of $20\,kW\,kg^{-1}$ has been developed [1].

Large capacitance ECs can be developed either by utilizing the so-called double-layer (d.l.) capacitance at electrode interfaces or employing the large redox pseudocapacitance that is developed at some transition metal oxide films (e.g.

* Corresponding author. Tel.: +1 613 562 5481; fax: +1 613 562 5170.
E-mail address: wpell@science.uottawa.ca (B.E. Conway).

0378-7753/$ – see front matter © 2005 Elsevier B.V. All rights reserved.
doi:10.1016/j.jpowsour.2005.06.002

RuO_2 [11], IrO_2 [12], Co_3O_4 [13]). To increase energy-density of ECs is a principal aim for promotion of EC performance. Since the energy-density of an EC, ED, increases with capacitance, C, and also the square of the operating voltage, ΔV, on charge, i.e. $ED = (1/2)q\,\Delta V = (1/2)C(\Delta V)^2$, a substantial improvement in energy-density can thus be achieved by either increase of capacitance by using high specific-area carbon materials or by increasing the operating voltage of an EC, using nonaqueous electrolytes instead of aqueous ones, thus corresponding to an increase of decomposition voltage from 1.0–1.5 V to 3 or 3.5 V or more, per cell unit. By combining all of the optimal conditions, a very large specific capacitance with large energy-density can be realized.

However, for ECs based on high specific-area porous carbon electrodes, some unavoidable opposing effects arise between the requirements for high ED and the necessities for very low internal resistance in order to maximize operating power density, PD. Thus, for future applications, it is of major interest for development of ECs currently utilizing porous C electrode materials, that better understanding of the relation of the pore-size distribution [14] to real specific-area values be gained in relation to distributed internal resistance, electrolyte wetting of the pores and the actually attainable capacitance. Additionally, study of rates of self-discharge and its mechanisms is of essential importance in evaluation of EC performance enabling the choice of materials that minimize self-discharge. The basic principles of such studies have been treated in earlier papers [1,5,15].

In the present paper, we examine quantitatively the requirements for performance evaluation of electrochemical d.l. capacitors, exemplified by results of studies on an high specific-area ($2500\,m^2\,g^{-1}$) woven C-cloth material (Spectracarb 2225) in aqueous H_2SO_4 at various concentrations, polarized at various rates under regimes of cyclic voltammetry and galvanostatic current-density variation. Special attention is directed to the effects of distributed capacitance and resistance in pores of the C material in relation to the de Levie signal-penetration effect [16] that determines how the measurable double-layer capacitance of porous C electrodes depends on sweep-rate in CV, current-density in charging curves and frequency in impedance spectroscopy. Additionally, the de Levie effect influences self-discharge behaviour in potential-decay and float-current measurements [5]. Notwithstanding the importance of extended cycle-life testing, even thermally accelerated, its lengthy duration prevented its adoption here.

2. Experimental

2.1. Configuration of electrodes for performance evaluations

Here, charge/discharge and polarization measurements are based on "single electrode" studies (i.e. half-cell EC electrodes) using both a separate counter-electrode and importantly a reference electrode. This procedure differs from that employed in most commercial tests which are made on two- or multi-electrode packaged devices, i.e. *without* a reference electrode, and can thus give more and direct information on the electrochemical behaviour of the tested C materials *separately* as cathodes or anodes.

2.2. Materials

Spectracarb 2225, C-cloth, having an high specific-area value of $2500\,m^2\,g^{-1}$ was obtained from Spectra Corp (Lawrence, MA 01840) and has the advantage of being able to be formed into electrodes having good mechanical integrity. High purity BDH Aristar H_2SO_4 was used as the electrolyte. Elsewhere [17], we have shown SEM photos of such electrodes from which it is clear that the main micro- and nano-scale real area arises within the individual fibrils of the cloth. Experiments were conducted in 0.01, 0.05, 0.5 and 5 M H_2SO_4 aqueous solutions after bubbling O_2-free N_2 in the usual way for deaeration.

2.3. Cell and instruments

An EG&G Parc M270 potentiostat/galvanostat, controlled by a computer with M270 software, was used to perform charge/discharge, self-discharge and float-current test experiments. All experiments were carried out in a three-compartment glass electrochemical cell, in the usual way, using the Spectracarb 2225 C-cloth as the working electrode; an hydrogen reference electrode and Spectracarb 2225 C-cloth was also used as the counter-electrode to ensure that the latter had larger area than the working electrode.

For open-circuit self-discharge and potential recovery, after respective anodic charging or cathodic discharging, to or from known controlled potentials, the declines or rises of electrode potentials after interruptions of charging or discharging currents, were followed by digital recording over four to five decades of time.

2.4. Preparation of the working C electrode

A piece of carbon cloth of known weight was first wrapped around a solid glass bead blown at the end of a glass tube (cf. ref. [18]), then secured by connection to a silver wire which was sealed within the glass tube. The current contribution at the connector wire was negligible due to its very small area ($0.063\,cm^2$) compared with that of the C-cloth ($8 \times 10^5\,cm^2$). The prepared working electrode was first wetted in the H_2SO_4 solutions; the resulting capacitative behaviour was reproducible and stable, even over several months.

3. Results and discussion

3.1. Charge and discharge behaviour

3.1.1. Cyclic voltammetry

Cyclic voltammetry is especially valuable and is the preferred method for studying double-layer capacitor materials

and resulting EC devices since it provides detailed information *directly* on the double-layer capacitance and its potential dependence, which is essential for examining the behaviour and structure of electrified interfaces. In cyclic voltammetry, current response, $i(V, t)$, at a scan rate $s = \mathrm{d}V/\mathrm{d}t$, gives the double-layer capacitance, $C = i/s$. The charge-density, q, accepted or delivered, is then obtained by integration, $q = \int \frac{i}{s}\,\mathrm{d}V$; the dependence of q on electrode potential, V, is then directly determinable as a differential quantity $C = \mathrm{d}q/\mathrm{d}V$. Such quantities always give more resolved information than corresponding integral charging-curve relations, i.e. total charge versus total potential. Hence, C is directly and conveniently evaluated as a $f(s)$ and potential by means of cyclic voltammetry, in the usual way. Correspondingly, C can also be directly evaluated as a function of frequency by impedance spectroscopy [19] and behaviour interpreted in terms of "*RC*"—ladder diagrams representing de Levie transmission line frequency response, as modeled by Miller, e.g. as in ref. [2].

The recorded voltammograms for sufficiently low s ($\leq$5 mV s^{-1}) and in the 5 M H_2SO_4 electrolyte approximate well to the behaviour expected for a pure capacitance (viz. capacitance-density becoming independent of sweep-rate and the anodic and cathodic curves are almost mirror-images of each other (Fig. 1), as also found for RuO_2 pseudocapacitor electrodes [20]). At higher sweep-rates, the voltammograms become distorted owing to increasing *iR*-drop, as is usually observed and treated in ref. [21]. The Spectracarb material exhibits a weak maximum in both the anodic and cathodic current responses around 0.4∼0.7 V, probably due to a pseudocapacitance contribution from surface functional groups, e.g. of the quinonoid type [22].

CV measurements can also usefully enable *C*-rates (in battery terminology) to be derived relative to a "full-charge" condition in aqueous medium, say at 1.2 V (RHE). The *C*-rate is then directly related to the sweep-rate s ($=\pm\mathrm{d}V/\mathrm{d}t$) V s^{-1} by *C*-rate = 3600 × s/1.2. Thus, it is seen that even relatively slow sweep-rates in CVs, e.g. s = 0.01 V s^{-1}, correspond to quite large *C*-rates, viz. 30*C* for this example. Hence, CV experiments on d.l. capacitors, at quite moderate s values, provide relatively high *C*-rate performance data in relation to those commonly quoted for operation of batteries, e.g. *C*/4 for Pb/acid. For the above reasons, it is easily seen why distortions of CVs are often significant for sweep-rates beyond 1–5 mV s^{-1}, even in well-conducting solutions.

Compared with those for 5 M H_2SO_4 solution, the CV curves for the C-cloth in dilute H_2SO_4 solutions (0.5, 0.05 and 0.01 M) deviate much more from ideal behaviour in their current responses (Fig. 2a and b). Deviations from ideality were especially marked in the CV responses either in low electrolyte concentration (<0.05 M) or at high scan rates. This is, as expected, due to increase of the *iR*-drop which arises principally from the complex internal distribution of resistance of electrolyte in porous electrodes (such as the C-cloth used in our present work) and is essentially different from the "equivalent series (solution) resistance" (ESR), R_s, at a planar

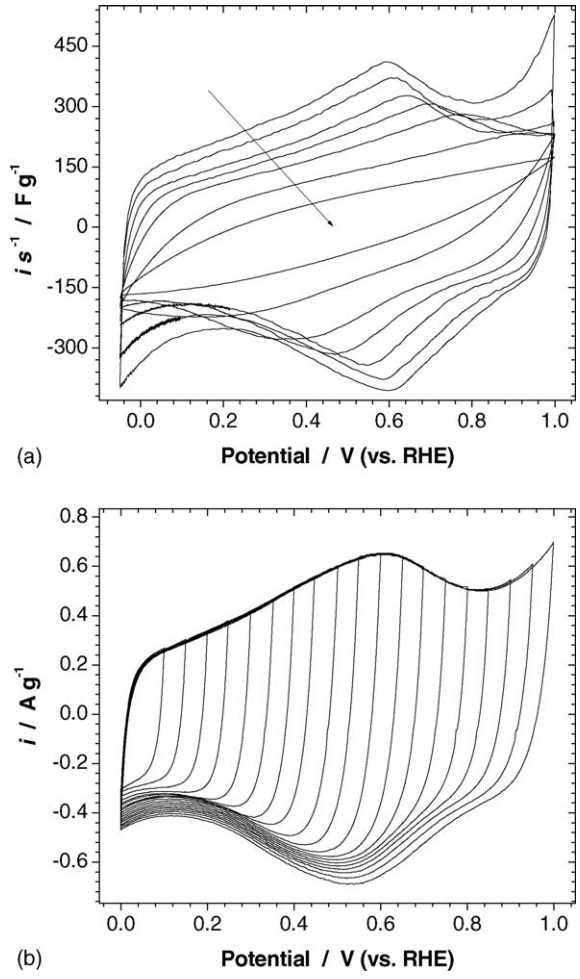

Fig. 1. (a) Cyclic voltammograms of the C-cloth electrode in terms of the capacitance response, i/s, in 5 M H_2SO_4 recorded between −0.05 and +1.0 V (RHE) for a sequential series of sweep-rates: 0.1, 0.5, 2, 5, 10, 25 and 50 mV s^{-1}. The arrow shows the direction of increasing sweep-rate. (b) A successive series of voltammograms, taken to progressively more positive potentials for a C-cloth electrode in 5 M H_2SO_4 at 2 mV s^{-1}.

one. It is well known that the *iR*-drop in a porous electrode is no longer single-valued at a given i, but increases down the pore since the local i decreases and the cumulative R increases due to a progressive increase of electrolytic resistance down the pore from its orifice resulting in the so-called "penetration depth", defined by de Levie [16], which decreases with rate in potentiostatic/galvanostatic measurements and with frequency in ac impedance techniques.

For a purely capacitative electrode, having zero R_s, both coulombic and energy efficiency (CE and EE) should be 100%. However, for an electrode having a real R_s, and hence unavoidable overvoltage, irreversible dissipative loss of energy density, ED, takes place, leading to EE < 100% since:

$$\mathrm{ED} = \frac{1}{2}CV^2 = \frac{1}{2}C\,[V(t) - iR_s]^2 \quad (1)$$

The coulombic $((q_A/q_C) \times 100)$ and energy efficiency $((\mathrm{ED_A}/\mathrm{ED_C}) \times 100))$ values for the C-cloth, determined as

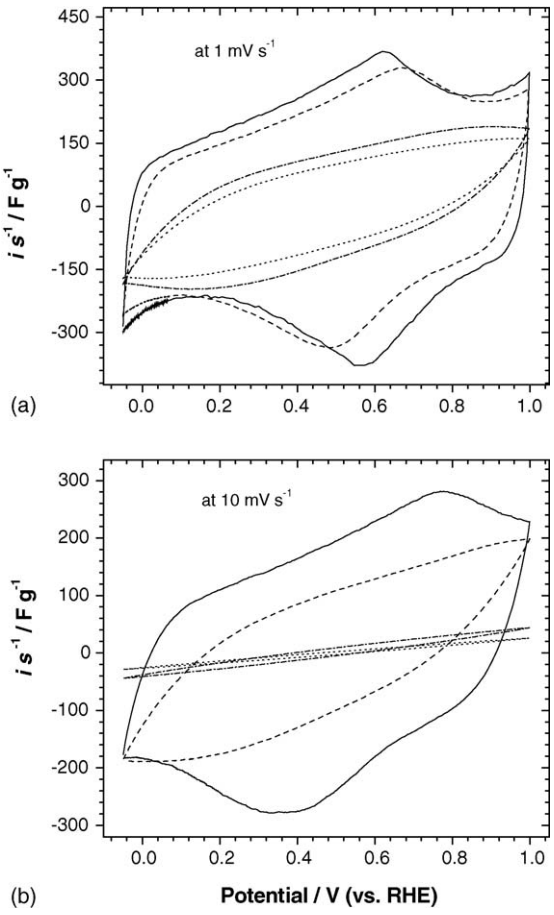

Fig. 2. Cyclic voltammograms of the C-cloth electrode for a series of H_2SO_4 electrolyte concentrations: 0.01 (···), 0.05 (- - -), 0.5 (- -) and 5 M (–), at 1 mV s^{-1} (a) and 10 mV s^{-1} (b).

a function of electrolyte concentration and scan rate (equivalent to charge/discharge rate) are listed in Table 1. The coulombic efficiency is rate-independent and approximates to 100%, while the energy efficiency is highly rate-dependent, decreasing from 78 to 36% in 5 M H_2SO_4 over range of $s = 0.5$–25 mV s^{-1}. As we have shown elsewhere [21], this is due to the *iR*-effect which increases with increasing *s*, leading to corresponding decreases in measured *C* (or *i*/*s*) (Fig. 3a). This is especially evident when the integral capacitance, determined over the 1 V potential range from experimental CV results, is plotted as a function of scan-rate (Fig. 3a) and/or electrolyte concentration (Fig. 3b). Similarly, the smallest energy efficiency and also its largest decrease (from 53 to 15%) arise in 0.05 M H_2SO_4 as compared with corresponding values in both 5 and 0.5 M H_2SO_4. Of course, this is because, as discussed earlier, R_s increases and (the accessible) *C* decreases significantly (Fig. 3b) with decreasing electrolyte concentration.

3.1.2. Galvanostatic charging and discharging

For practical testing of supercapacitors or batteries, the complementary procedure of recording charge/discharge relations at constant-currents is usually employed. This method also usefully provides information (see Section 3.2) enabling construction of Ragone plots [23] to be made, relating achievable EDs to operating PDs. Such relations provide essential performance parameters for practical evaluation of capacitors or their constituent single electrodes.

Theoretically, for a constant capacitance device without distributed resistance, the constant-current charge and discharge relations are straight lines with slopes $+1/C$ and $-1/C$, respectively. The total charge, q_T, is independent of charging current-density, and both coulombic and energy efficiencies are, for such conditions, 100%. For practical

Table 1
Charge and energy parameters calculated from cyclic voltammetry at the C-cloth electrode for three electrolyte (H_2SO_4) concentrations[a]

Concentration (M)	*s* (mV s^{-1})	q_+ (C g^{-1})	q_- (C g^{-1})	Coloumbic efficiency (%)	ED_+ (W s g^{-1})	ED_- (W s g^{-1})	Energy efficiency (%)
5	0.5	354	349	99	199	152	78
	1	337	336	100	191	146	76
	2	323	322	100	185	138	75
	5	288	298	103	178	120	67
	10	267	271	101	171	97	57
	25	211	207	98	149	54	36
0.5	0.5	324	322	100	188	132	70
	1	302	302	100	179	119	66
	2	278	279	100	171	103	60
	5	228	225	99	153	66	43
	10	171	169	99	126	38	31
	25	91	88	97	73	14	19
0.05	0.5	213	216	101	135	72	53
	1	170	176	103	118	46	39
	2	122	128	105	92	26	28
	5	62	63	102	50	10	20
	10	33	33	99	27	5	19
	25	14	14	95	12	2	17

[a] Potential limits: −0.05 to 1.0 V.

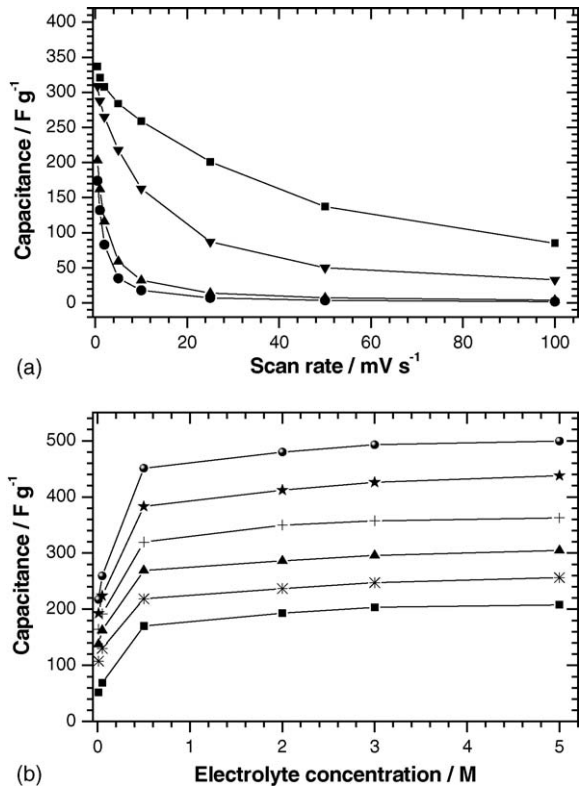

Fig. 3. (a) Variation of integral capacitance over the potential range of −0.05 to 1.0 V (RHE) with scan-rate and electrolyte concentration: 0.01(●), 0.05 (▲), 0.5 (▼) and 5 M (■). (b) Capacitance at various potentials: +0.1 (■), +0.2 (*), +0.3 (▲), +0.4 (+), +0.5 (⋆) and +0.6 V (◒), as a function of electrolyte concentration determined from cyclic voltammetry data at 0.1 mV s^{-1}.

devices having significant ESR and/or potential dependent capacitance, the charge/discharge curves will deviate, however, from straight lines and initially, on charge and at the point of reversal of the direction of current to discharge, ohmic potential drops observably arise, causing a shift and asymmetry of the charge/discharge profiles. Then the coulombic and especially energy efficiency will be less than 100%.

Constant-current charge and discharge behaviours of the C-cloth electrode, studied in 0.01, 0.05, 0.5 and 5 M H_2SO_4 at 1, 1.5, 2.5, 5, 10 and 50 mA, are shown comparatively in the series of Fig. 4a–d, in which are plotted the voltage responses as a function of charge, Q. For these curves, the potential versus Q relations exhibit, as expected, non-linearity, dependent, in part, on the charging/discharging current, indicating that the capacitance of the C-cloth, as measured, is not constant over the potential ranges in charge and discharge as also indicated by the CV curves (Fig. 1). This must be a result of several effects: (a) that of the direct ESR; (b) and of redistribution of charge within the pores of the 3-D C-cloth structure during charging or discharging; (c) any pseudocapacitance contribution due to redox-active surface groups. Simulation results (which provided the same characteristic curves) from polarization of a five-element series-parallel hardware network of appropriately valued capacitors and resistors [24] confirms the first two effects while the CV curves shown, as above, reflect some contribution from the (c) effects. Also, further support is provided by the following interesting observations:

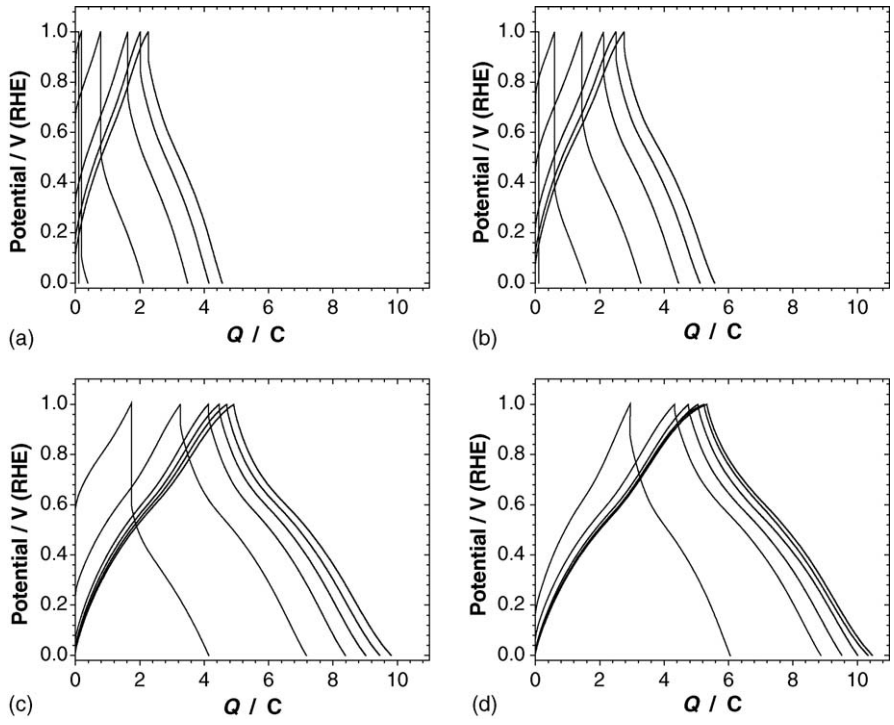

Fig. 4. The potential response to constant charging/discharging currents of 1, 1.5, 2.5, 5, 10 and 50 mA as a function of charge (a–d) for a C-cloth electrode in a series H_2SO_4 electrolyte: 0.01 (a), 0.05 (b), 0.5 (c) and 5 M (d). Accepted/delivered charge increases with decreasing charging/discharging current.

(i) The accepted and delivered charges are substantially decreased with increasing current for each case of the H_2SO_4 solutions indicating clearly the effect of the distributed (electrolytic) resistance on acceptance or delivery of charge under conditions of increasing rate of charge or discharge. This effect becomes, of course, diminished with increasing electrolyte concentration due to diminishing resistivity within the pores (compare Fig. 4a–d).

(ii) A significant initial, rate-dependent drop/rise in potential is observed, indicating the presence of a significant ESR (Fig. 4a–d). The derived *iR*-drop on discharge increases as the concentration of electrolyte decreases and, of course, is most significant for the lowest concentration of 0.01 M and for the largest rate of charging/discharging (Fig. 4a). Note, however, the serious *iR*-drops on discharge as a function of H_2SO_4 concentration and discharge/charge current, which arise for electrolyte concentrations less than 0.5 M. Thus, the *iR*-drop and the "potential redistribution effect" [24] for the high-area porous electrode material are, as expected, significantly decreased in H_2SO_4 solutions at concentrations >0.5 M.

(iii) The accessible capacitance of the C-cloth electrode increases with increasing concentration of electrolyte and with decreasing charging/discharging rate. This is consistent with the results of cyclic voltammetry (Figs. 1 and 3) and can be attributed to the more effective penetration of current and better electrolyte conductivity down the pores, leading to increases of the electrochemically chargeable area of the C-cloth electrode and consequent increases of capacitance and thus of storable energy. Thus, decreasing charging/discharging rate and increasing H_2SO_4 concentration minimize the potential redistribution effect (cf. ref. [16]).

(iv) At high charge/discharge rates (or in CVs at high sweep-rates), the current response may simply come from that of the pore orifices, i.e. the outer layers of the C-cloth electrode fibres due to insufficiency of time for signal penetration [16] into the pores, while low rates ensure that the modulation signal can penetrate into pores (especially intra-fiber nano-scale pores) causing larger current, hence charging, response. How large is the current response change depends on how deep the signals penetrate and how large is the distributed resistance within and outside the pores, which is, of course, dependent also on the concentration of electrolyte.

Fig. 5a and b show how the charge acceptance, the energy and their efficiencies vary with electrolyte concentration under galvanostatic charge and discharge conditions. The charge and energy increase with increasing electrolyte concentration and also with decreasing charge/discharge rate, indicating deeper penetration of the signal into the pores and thus more accessibility for charging of inner areas of the C-cloth electrode under such conditions. The coulombic and energy efficiencies show, however, different dependency on variation of charge/discharge rate and electrolyte concentration. Coulombic efficiency is independent of rate (Fig. 5a) and remains relatively constant at approximately 100%. Changing electrolyte concentration also has no effect on coulombic efficiency, which still maintains a value of near to 100%, a matter of practical significance. This indicates that (a) the effects of charge/discharge rate and electrolyte concentra-

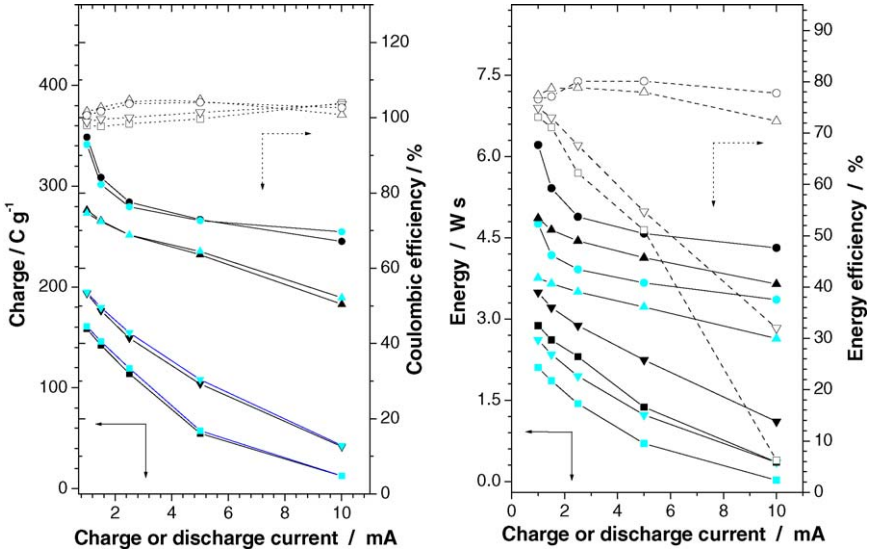

Fig. 5. (a) Charge (solid lines and symbols) and coulombic efficiency (dotted lines and empty symbols) changes as a function of charge/discharging current for different H_2SO_4 electrolyte concentrations: 0.01 (square), 0.05 (down triangle), 0.5 (up triangle) and 5 M (circle). Solid symbols represent charge and grey symbols the discharge responses. (b) Changes of energy (solid lines and symbols) and energy efficiency (dotted lines and empty symbols) as a function of charging/discharging current for H_2SO_4 electrolyte at various concentrations: 0.01 (square), 0.05 (down triangle), 0.5 (up triangle) and 5 M (circle). Solid symbols represent energy for the charge and grey symbols the discharge processes.

tion on the acceptance and delivery of charge are comparable over the potential range of this study and (b) full delivery of the accepted charge in each of the cases is possible. 100% (or near) coulombic efficiency, evaluated over the whole voltammogram, is not, however, an indication of electrochemical reversibility. Coulombic inefficiencies result when some portion of the charging current is lost to parasitic reactions, e.g. gas evolution on overcharge.

The energy efficiency, EE, is, however, highly rate and electrolyte-concentration dependent and much less than 100%, especially for low electrolyte concentrations, e.g. 0.05 and 0.01 M (Fig. 5b). The charge/discharge processes are subject to the effects of iR, concentration and, in the case of Faradaic pseudocapacitance, activation polarization. Each of these polarization components increases with increasing current-density or rate and, as a result, increases the overall voltage on charge or decreases it on discharge. Hence, the energy efficiency, which is a function of the ratio of voltage on discharge to that on charge, over a given potential range, can exhibit significant dependences on both electrolyte concentration and rate, as seen in Fig. 5b.

3.2. *Ragone plots (power-density versus energy-density relations)*

It is interesting, useful and essential, for comparative evaluation of electrochemical power sources, to evaluate PD and ED relations (Ragone relations) for battery or capacitance devices, especially for an asymmetric device consisting of an hybrid combination of high PD EC and high ED battery–electrodes, e.g. see ref. [24]. Power and energy balancing in the coupling between these two components is an essential requirement and can be derived from Ragone plots. Note, however, that the factors that determine the ED versus PD relations for ECs are different, in a major way, from those for batteries because, on discharge, an intrinsic feature of a charged EC is a decline of its voltage with state of discharge, determined by $C = \mathrm{d}q/\mathrm{d}V$ while, for an ideal battery, the cell voltage remains almost constant. Thus, since for a capacitor, the voltage during discharge declines, corresponding to withdrawal of charge per gram, q, both ED (Eq. (1)) and PD ($=iV$) must also fall with increasing state-of-discharge, i.e. they both depend on state-of-charge (SOC) of the electrode giving Ragone plots that depend on both the rate, i, and the state-of-discharge.

A series of plots of PD versus ED-available (Fig. 6) were made as a function of state-of-charge of the C-cloth electrode for rates of 1–50 mA in four electrolyte concentrations from 0.01 to 5 M. The experimental curves of PD versus ED-available in 5 M electrolyte (Fig. 6d) clearly show the fundamental features of ECs, i.e. both PD and ED-available decline almost linearly with decreasing SOC. The plots deviate from linearity with decreasing electrolyte concentration (compare Fig. 6a–d) due to the "penetration depth" and "potential redistribution" effects, discussed above. Available ED also increases, as expected, with increase of electrolyte concentration. For basic reasons, PDs always significantly decrease with decreasing rate, i, as found for each of the four electrolytes indicating how substantial effects of rates of charge delivery/acceptance determine the performance of ECs. In the high-concentration electrolyte solutions ($\geq$0.5 M), ED-available is relatively independent of delivery rate when

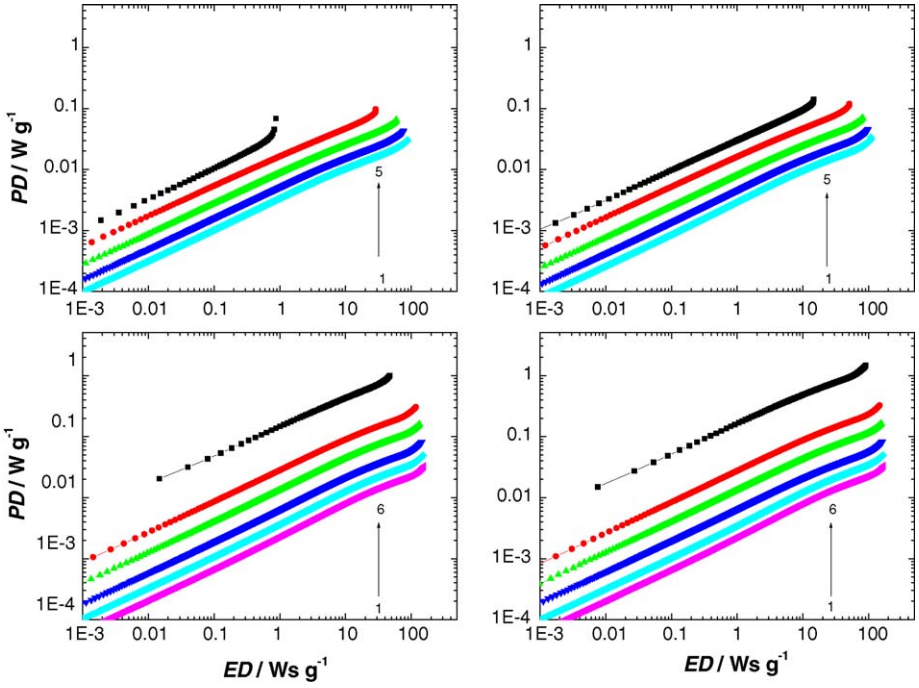

Fig. 6. PD vs. ED for various current-densities: (1) 1 mA (►), (2) 1.5 mA (♦), (3) 2.5 mA (▼), (4) 5 mA (▲), (5) 10 mA (●) and (6) 50 mA (■) in four electrolyte concentrations—(a) 0.01 M, (b) 0.05 M, (c) 0.5 M and (d) 5 M. Arrows indicate direction of increasing current.

$i < 5$ mA (Fig. 6c and d) whereas, in more dilute electrolyte, the ED is much more dependent on rate (Fig. 6a and b). Significant ED is hardly realizable for $i > 10$ mA in 0.01 M electrolyte (Fig. 6a) but shows excellent performance values for 5 M electrolyte (Fig. 6d). Note that the PD versus ED-available curve cannot be recorded at a rate of 50 mA in 0.01 and 0.05 M solutions (Fig. 6a and b) due to high solution resistivity, but does exhibit good shapes in 0.5 and 5 M (Fig. 6c and d). Generally, in dilute electrolyte solutions (0.01 and 0.05 M), increasing delivery rate substantially decreases the ED, while for high electrolyte concentrations (0.5 and 5 M), effects of delivery rate on PD are relatively more apparent than at low concentrations (Fig. 6a and d). Of course, operation of a practical electrochemical capacitor is limited to the voltage range V_i to $V_i/2$ (i.e. 75% of the total energy stored has already been delivered and at constant-current, the time to recover the first 75% of the total energy stored is the same as that for the remaining 25%). Significantly, Fig. 6 illustrates the decline in power with state-of-discharge (declining voltage).

The construction of Ragone plots at 100% SOC from the experimental data in Fig. 6 for these four electrolytes is shown in Fig. 7 for six delivery rates. The PDs of *fully charged* electrodes are plotted as a function of the ED of the electrode at each of the six delivery rates (i.e. the maximum power-density at that rate and electrolyte concentration is plotted as a function of energy-density). It is important to remember that the PD will decrease for each electrolyte concentration and rate as the electrode becomes progressively discharged (SOC effect referred to above and illustrated in Fig. 6).

Nevertheless, trends in PD and ED evident at the initial SOC of 100% are maintained as the electrode discharges. Obviously, both PD and ED significantly increase with increase of electrolyte concentration from 0.01 to 5 M as shown in Fig. 7 for the initial SOC of 100%. For a given electrolyte, however, PD increases but ED necessarily decreases with increasing delivery rate, i.e. higher delivery rates always correspond to higher PD at the expense of lower EDs, while lower delivery rates give lower PDs and higher EDs. Note, especially for the electrode in 0.01 M H_2SO_4, that significant decrease in ED at high rate (5 and 10 mA) is not accompanied by an increase in PD (Fig. 7). The best performance of the C-cloth electrode is achieved in 5 M electrolyte solution since the high concentration (low resistivity) of the electrolyte ensures minimal *iR*-losses and maximum penetration of the charge/discharge signal into the pores of the carbon electrode and hence maximum energy-storage capability (see Fig. 7).

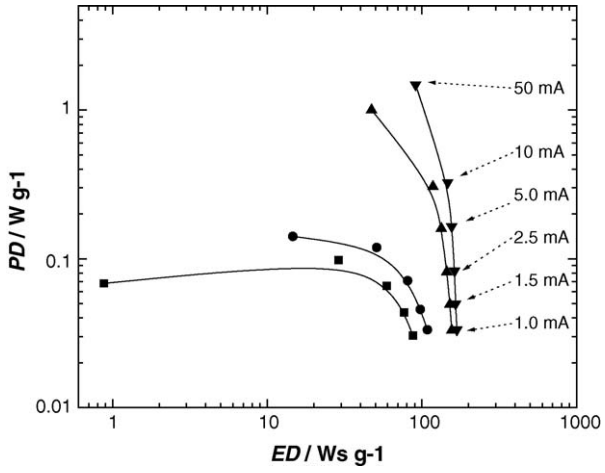

Fig. 7. Ragone plots for the fully charged C-cloth electrode for various constant currents as marked on the figure for four electrolyte concentrations: 0.01 M (■), 0.05 M (●), 0.5 M (▲) and 5 M (▼).

3.3. Self-discharge

Self-discharge is a common phenomenon in the behaviour of electrical charge-storage devices such as batteries or electrochemical capacitors, and is defined in terms of the rate of decline of voltage of an electrochemical power source [1] with time, t, on open-circuit following charging. Since self-discharge involves a decline of potential (V) with time at a single electrode or of ΔV between the electrodes of a charged device, it must also lead to a decline of available electrical energy as indicated by Eq. (2) for an electrochemical capacitor:

$$(\mathrm{ED})_t = \frac{1}{2}C(\Delta V)_t^2 = \frac{1}{2}q(\Delta V)_t \tag{2}$$

Hence, the rate of energy loss will be determined by the rates of decline of cell voltage, ΔV_t:

$$\frac{\mathrm{d}(\mathrm{ED})_t}{\mathrm{d}t} = \frac{C}{2}\frac{\mathrm{d}[(\Delta V_t)^2]}{\mathrm{d}t} = C\,\Delta V_t \frac{\mathrm{d}(\Delta V_t)}{\mathrm{d}t} \tag{3}$$

Thus, it is obvious that self-discharge behaviour is of major practical importance for device-performance specifications, especially in stand-alone or stand-by applications.

Generally, an ideal, non-leaky capacitance never suffers self-discharge which can only occur if some Faradaic electron-transfer processes, e.g. "shuttle reactions" [15], take place due to the existence of impurity or reactive species/groups arising from materials used within the device or due to some ohmic leakage. Thus, self-discharge rates can vary extensively depending on the chemistry and electrochemistry of the system, the provenance of high-area C materials and their pretreatment, the purity of the reagents and electrolyte, the absence of oxygen, cleanliness of device fabrication procedures and the temperature. The actual rates are determined by the mechanisms of the processes by which the self-discharge takes place, as treated in our ref. [15] where three kinetic cases were examined giving rise to diagnostic criteria for distinction of such processes. They can be summarized as follows:

(a) When self-discharge is caused by a non-diffusion-controlled Faradaic process associated with reduction or oxidation of either the products from overcharge or redox-reaction impurities such as Fe^{2+}/Fe^{3+}, solution

oxygen, etc., the decline of voltage, V, versus $\log t$ would give a straight line:

$$V_t = V_i - A \log(t + \theta) \quad (4)$$

where θ is an integration constant arising in the mathematics (see ref. [15]).

(b) If self-discharge is due to a semi-infinite, diffusion-controlled Faradaic process involving impurities at a planar electrode, the potential would decline with square-root of t, viz:

$$V_t = V_i - \frac{2z\mathrm{FAD}^{1/2}\pi^{1/2}c_0}{C} t^{1/2} \quad (5)$$

(c) If self-discharge arises from "short-circuit" leakage between one electrode and another, e.g. as in a faulty bipolar cell, $\ln V_t$ versus t would follow a linear relationship:

$$\ln V_t = \ln V_i - \frac{t}{RC} \quad (6)$$

where R is an adventitious ohmic load resistance, e.g. in a leaky bipolar configuration.

The electrochemical kinetic behaviours described in Eqs. (4)–(6) are easily distinguishable from each other and thus provide a diagnostic basis (treated in ref. [15]) for identifying self-discharge mechanisms after recording the time-dependent voltage of an electrode or a cell on open-circuit (see results below) over a sufficient range (several decades) of time, t.

Presence of impurities, including but not limited to water in organic electrolyte configurations, has been identified as the cause of self-discharge and leakage current in electrochemical capacitors [25–27]. Self-discharge has been linked to carbon functionality and to the accessibility of the microporous surface area [28]. In an attempt to control and limit the extent of self-discharge researchers have considered the effects of varying the electrolyte composition [27,29], nature of the conducting agent employed in the electrode [30], as well as by the composition of the separator material [31].

Two procedures are now employed for characterizing self-discharge behaviours of electrochemical capacitors and batteries. One is to follow the time-dependent voltage decline to distinguish the self-discharge mechanism and to derive kinetic data on open-circuit as described above. The other procedure is the so-called "float current" measurement in which a constant potential for a single electrode or ΔV for a cell is applied in order to record the resulting float current, i_f, that is required to maintain that V or ΔV constant. Then, i_f must be equal to the self-discharge rate that would be arising at that potential.

3.3.1. Self-discharge behaviour of the C-cloth electrode

Self-discharge experiments using the C-cloth electrode were conducted in 5 and 0.5 M H_2SO_4 by applying constant-current charging up to various potential values then interrupting the polarization current to record open-circuit potential decays with time. The resulting data, plotted either as $\ln V_t$ versus t or V_t versus $t^{1/2}$, are not linear, showing that self-discharge is not due to a linearly diffusion-controlled Faradaic process nor to discharge into an adventitious load resistance (cf. Eqs. (5) and (6)). However, plots of V_t versus $\log t$ do exhibit straight lines after $t \gg \theta$ (Eq. (4)) as shown in Fig. 8. This is consistent with the mechanism of case (a) (Eq. (4), referred to above), corresponding to a non-diffusion-controlled Faradaic process.

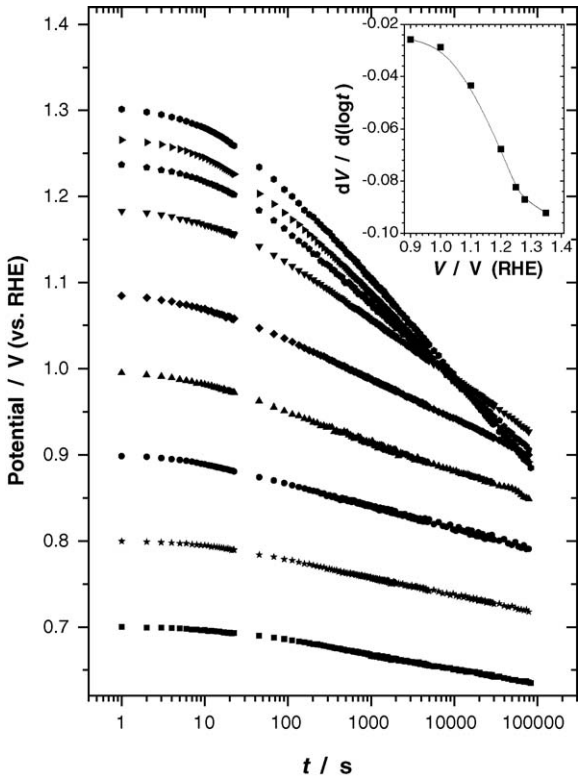

Fig. 8. Potential-decay relations for self-discharge at a single C-cloth electrode, vs. RHE, initiated from a *series of potentials*: +0.7 (■), +0.8 (⋆), +0.9 (●), +1.0 (▲), +1.1 (♦), +1.2 (▼), +1.25 (⬟), +1.28 (►) and +1.35 V (⬢), in 5.0 M H_2SO_4 after positive charging at 10 mA. Inset: $dV/d(\log t)$ as a function of the initial potential for the series of potential decay curves shown here in this figure.

Although the V_t versus $\log(t+\theta)$ relations (Fig. 8) are linear over several decades of t for all recorded plots, it is important to notice that the *slopes* of these open-circuit potential plots ($dV_t/d(\log t)$) are dependent on the initial potential, V_i or initial state-of-charge in contrast to the behaviour predicted by Eq. (4). The slopes decrease with decreasing initial polarization potential (inset in Fig. 8), eventually becoming potential independent when $V_i \leq +0.9$ V, which is just the onset of rapid potential rise in the CV curve (cf. Fig. 1a, at low scan rate). Since the beginning of the rapid potential rise is related to the starting of *non-capacitative charging* of the C-cloth electrode and the slopes of the V_t versus $\log(t+\theta)$ plots tend to be almost the same value below that potential, the slope change therefore must arise, at least in part, from

non-capacitative behaviour of the electrode. This is clearly evidenced by the behaviour in Fig. 8 where larger changes of slope arise following higher initial polarization potential.

The above behaviour is to be contrasted with that of the nickel-oxide electrode (cf. ref. [32]) where the time-dependent positive potentials, V_t, recorded from several different V_i values, converge to a *common plot* of V_t versus $\log(t+\theta)$, i.e. when the values of the integration constant θ (Eq. (4) and ref. [15]) are properly included in the data-processing procedure. This difference from the behaviour at porous C is attributable to the fact that the self-discharge process at the Ni·O·OH electrode is mainly from the redox pseudocapacitance of its external surface associated with measurable O_2 evolution [32], i.e. there is relatively little influence of the de Levie "porous-electrode effect".

Actually, in the case of C due to its highly porous structure and its resultant complicated charge/discharge behaviour, the slope of V_t versus $\log t$ (in Eq. (4)) is not only related to the Tafel slope of the self-discharge reaction, but is also possibly influenced by the potential-dependence of the capacitance itself. This is reflected in Fig. 8. When over-charge evolution of O_2 occurs, the capacitance of the electrode changes due either to the change of state-of-charge and/or the change of the electrode's surface state, including but not limited to variation of the surface functional groups of the C material; the latter effect may be the result of damage to or breakage of bonding of the C material, as has been reported in the literature [33,34], leading to subsequent increase of the *iR*-drop. The higher the overcharge, the more serious are such effects which therefore have practical significance. This may account, in part, for the slope changes of V_t versus $\log(t+\theta)$ plots with changes of V_i.

The logarithmic decay slope was also found to be a function of the magnitude of the charging current, as shown in Fig. 9 in which V_t versus $\log t$ plots are recorded after charging a C-cloth electrode at a series of current values (0.1, 2, 5, 10 and 50 mA) but to the *same initial potential*, 1.1 V, followed by open-circuit decay. These plots may be divided into three distinct regions: short times, <2 s; intermediate times 2–100 s (dependent on the rate) and long times, >100 s. The initial potential drop at short times, <2 s, i.e. from 1.1 V to ca. 1.095, 1.075, 0.995, 0.875 and 0.745 V for 0.1, 2, 5, 10 and 50 mA charging currents, respectively, may be attributed, primarily, to *iR*-polarization effects of solution resistance.

Of more significant interest, Fig. 9 clearly shows that the slopes of the logarithmic decay curves at long time, >100 s, decrease with increasing charging current. In addition to differences in the extent of *iR* polarization due to solution resistance, different charging-currents corresponding to different charging-rates will establish different "penetration depths" down the pores. As a result, time-dependent distributions of charge in the distributed double-layer at the extended pore surfaces will be dependent on charge-rate hence causing changes in apparent capacitance, consequently leading to differences of slopes of V_t versus $\log t$ (cf. ref. [15]).

At lower charging-currents, it is supposed that the charge can be distributed amongst both the outer and inner surfaces of the C-cloth electrode. At higher current-densities, the charge/discharge arises mainly at the surface of outer regions of the electrode structure. Hence, the extent of self-discharge resulting from the charge redistribution effect within the electrode itself will be greatest for high-rate charging resulting in more rapid drop of potentials at intermediate times (2–100 s) for electrodes charged at high currents (50 and 10 mA, cf. behaviour for 0.1 mA, Fig. 9).

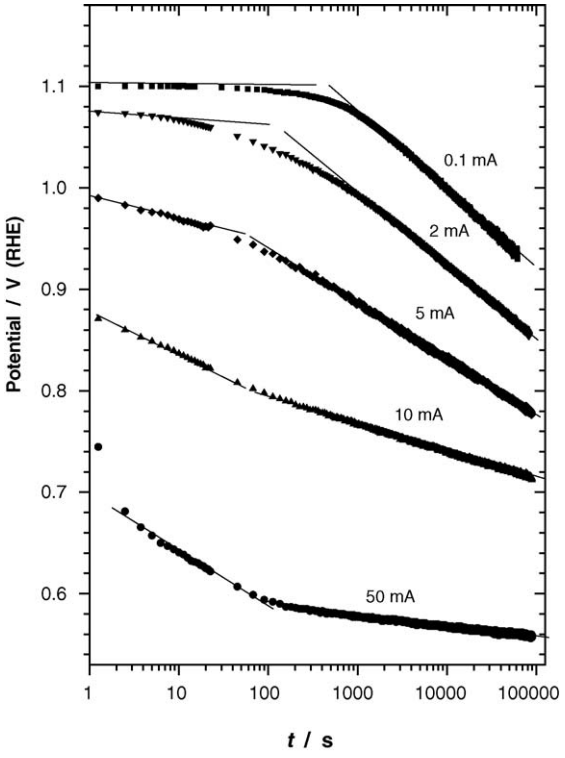

Fig. 9. Potential-decay relations for self-discharge as in this figure initiated at the *same potential* +1.1 V in 0.5 M H_2SO_4 after charging at a series of charging currents: 0.1 (■), 2 (▼), 5 (◆), 10 (▲) and 50 mA (●).

Interestingly, and consistent with the above interpretation, analogous phenomena of *potential recovery* are observed when the C-cloth electrode is polarized cathodically to various potentials and then allowed to relax on open-circuit. The resulting potential recovery (V_r) is found also to be approximately linear with $\log t$ (Fig. 10), just like that for self-discharge, and the slopes of V_r versus $\log t$, corresponding to rates of potential recovery, are again dependent on state-of-charge. The less positive is the polarization potential prior to open-circuit recovery (Fig. 10), the greater is the rate of potential recovery. It should also be noted that the charge/discharge history of the C-cloth electrode, e.g. the maximum potential to which the electrode had previously been polarized, also influences the rate and extent of potential recovery. This is shown in Fig. 11 for the C-cloth electrodes that had been polarized to different initial potentials and then discharged at the same current of −1.0 mA to the same final potential of +0.1 V RHE; *different* recovery rates are exhibited, dependent on the initial polarization potential. The higher the initial potentials prior to discharge, the greater are the rates of poten-

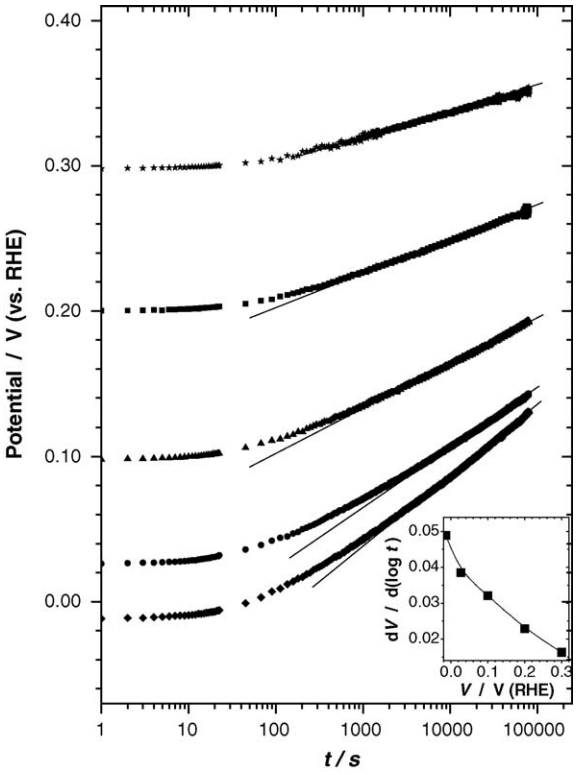

Fig. 10. Potential-recovery relations at the C-cloth electrode initiated from a series of increasing potentials in 5.0 M H_2SO_4. The inset shows slopes of the V vs. $\log t$ relations as a function of the initial polarization potential at the C-cloth electrode, as in Fig. 8.

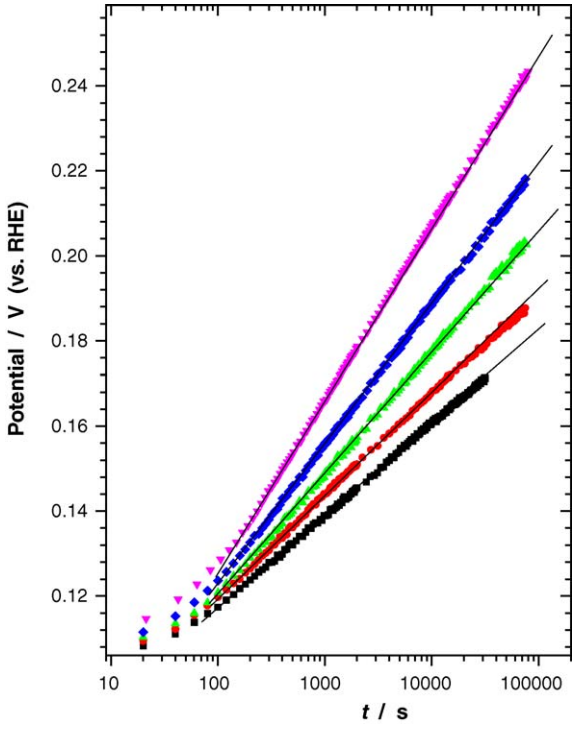

Fig. 11. Potential-recovery relations at the C-cloth electrode recorded after discharging from a series of polarization potentials, +0.5 (■), +0.7 (●), +0.9 (▲), +1.1 (♦) and +1.25 V (▼), down to the same final potential, +0.1 V, in 0.5 M H_2SO_4.

tial recovery. This phenomenon is again attributable to the effects of redistribution of surface charge in the porous C-cloth material as was demonstrated with hardware *RC* model circuits in ref. [24].

3.3.2. *Float-current measurement behaviour*

Theoretically, float-currents recorded at a certain potential at a planar electrode should remain constant in time (after the initial, short d.l. charging transient), matching the spontaneous self-discharge current passing at the potential, thus maintaining the electrode (or cell) at its initial state-of-charge. Experimental measurements were made by potentiostatically polarizing the C-cloth electrode to a series of potentials, V, from +0.6 to +1.1 V, and recording the float-current, i_f, which is found to decay for over 3600 s. Interesting information is obtained from the data in Fig. 12a–c which can throw new light on the nature of the self-discharge at the porous, high specific-area C-cloth (or other porous C materials), as discussed below.

The first distinguishable aspect of float-current behaviour at the C-cloth electrode is the long, potentiostatic transition time, from 20 to 300 s depending on applied potential and also on electrolyte concentration, which is quite different from that, μs to ms time scales, in potential-step experiments at plane electrodes. This, we believe, is due to two factors. The first is again the de Levie charge redistribution effect usually arising at porous electrodes [16] which behave in essentially different ways from a common plane electrode in terms of charge or current distribution. In a porous material such as the C-cloth electrode, as we have emphasized, the *iR*-drop is not constant but varies down the pores. This leads to a "penetration-depth" dependent distribution of accessible double-layer capacitance which, coupled with such pore-depth dependent solution resistance, constitutes a complicated "*RC*" network [2,16,24]. Then any potential or charging/discharging signal does not have an immediate and uniform charging effect on the whole electrode matrix, i.e. no unique *RC* time-constant will apply immediately, but time is required for charge to become redistributed ultimately to a uniform state-of-charge of the electrode (or a cell). Theoretical calculations based on the work of Posey and Morozumi [35,36] demonstrate that response time for a porous electrode is significantly longer than that for a planar electrode having equivalent capacitance and most significantly that while the log of the capacitor charging current following a potential step experiment for a planar electrode declines linearly with time, it does not for a porous electrode even when no self-discharge process occurs.

Such behaviour was demonstrated experimentally with the five-element hardware circuit created in ref. [24]. The "penetration depth" actually corresponds to a distribution of depth to which the charging or potential signal can penetrate the pores and is dependent on the electrolyte conductivity and diameter/shape of the pores. Hence, the effective *RC* "product" for high electrolyte concentrations is smaller than that for lower electrolyte concentrations, leading to decreases

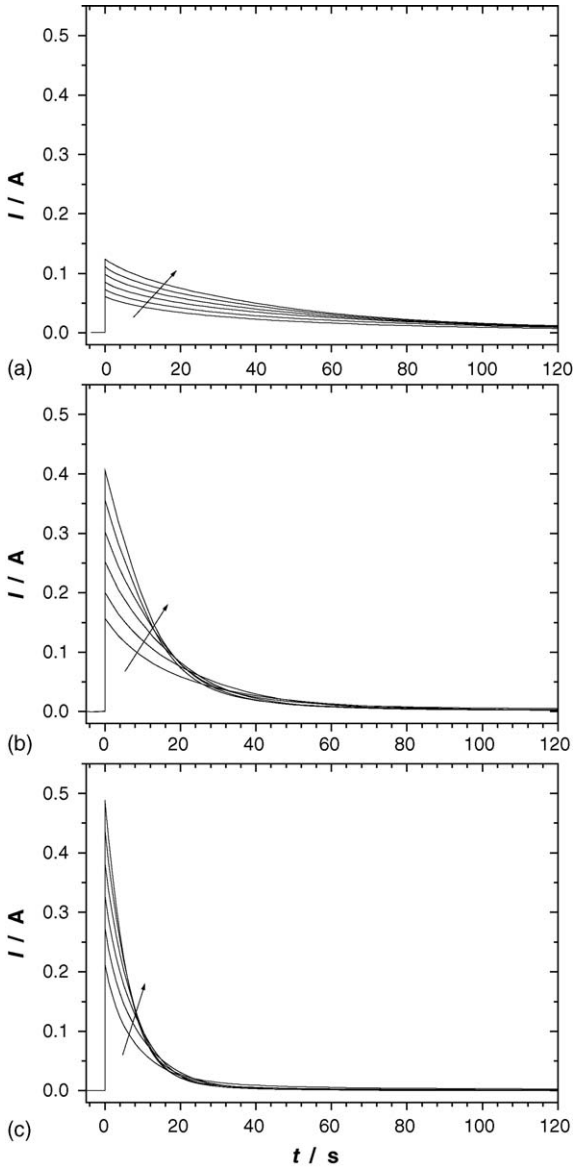

Fig. 12. Potentiostatic float-current responses recorded at the C-cloth electrode in three electrolytes ((a) 0.05 M, (b) 0.5 M and (c) 5 M) from six polarization potentials (+0.6, +0.7, +0.8, +0.9, +1.0 and +1.1 V, RHE) for durations 0–3600 s (figures show curves from 0 to 120 s region). Arrows show directions of increasing initial anodic polarization potentials.

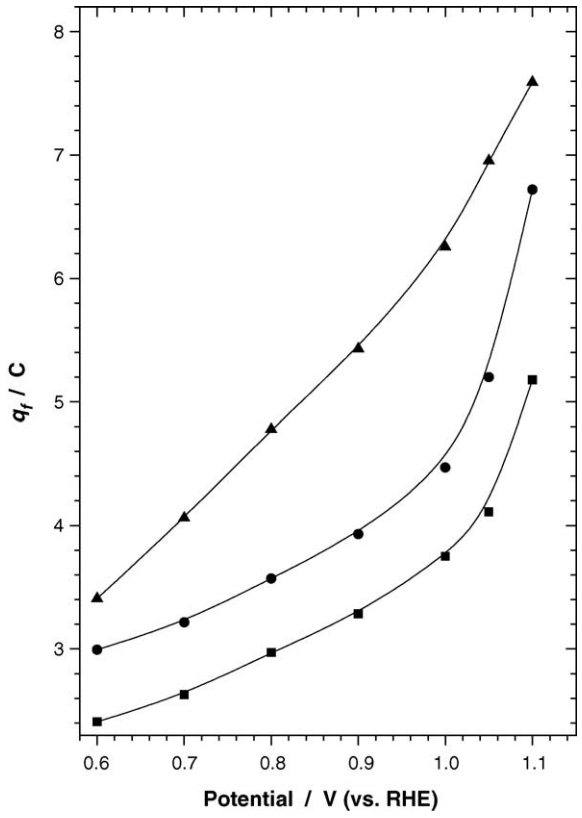

Fig. 13. Accumulated charge, determined from float-current experiments shown in this figure plotted as a function of polarization potentials in 0.05 M (▲), 0.5 M (●) and 5 M (■) H_2SO_4.

of potentiostatic transient times with increasing electrolyte concentration as indicated in Fig. 12a–c. The second factor that causes the large difference in transient charging times between the porous C-cloth electrode and a common plane electrode is, of course, the well known, very much larger (but rate-dependent) capacitance of the C-cloth electrode than that of plane electrodes of the same superficial area.

The two most interesting parameters in float-current measurements are the float-current, i_f, and the accumulated charge, q_f, at various potentials in the range corresponding to self-discharge. i_f, as expected, is required to balance the self-discharge rate, while q_f represents the extents of charge that have to be passed into (or from) the porous C-cloth electrode surface to establish a steady-state of accommodated double-layer charge at a given potential, associated with a steady self-discharge or potential-recovery current or rate. Hence, q_f would reflect the extent of self-discharge for porous, high specific-area C materials. Fig. 13 shows the q_f versus V curves obtained by integration of the i_f versus t transients that arise from potentiostatic polarization to various potentials as exhibited in Fig. 13a–c over the time scale of 0–3600 s. Note that q_f increases with both increasing polarization potentials and decreasing electrolyte concentrations, indicating the increase of self-discharge rate at both higher polarizing potential and lower electrolyte concentration. These results are consistent with the open-circuit potential decay/recovery results discussed in Section 3.3. The rate of self-discharge increases with V_i and also with decreasing electrolyte concentration (see Figs. 8 and 10 cf. Fig. 9).

It is also interesting to note from Fig. 13 that q_f shows the expected slow increase over the potential range of +0.6 to +1.0 V, but an unexpected, more rapid rise is seen when $V > +1.0$ V, especially in higher (0.5 and 5 M) electrolyte concentrations (Fig. 13). This is obviously an indication of a mechanism change in the self-discharge process which occurs again in the same potential range as that corresponding to the rapid current rise in the CV curve (cf. Fig. 1a), most probably due to onset of non-capacitative charging of

the C-cloth electrode, related to O_2 evolution and/or electrochemical damage to the C-cloth (see discussion below).

Another interesting feature of the float-current behaviour of the C-cloth electrode is the initial float-current magnitudes (at $t = 0$) and the shape of i–t curves over the duration of the potentiostatic transient. It is suggestive that two parameters reflect the "accessible area" of the porous, high specific-area C electrodes. This supposition is supported by the float-current responses of the C-cloth electrode in H_2SO_4 at different concentrations shown in Fig. 12a–c. It is clear that for higher H_2SO_4 concentrations, corresponding to larger "penetration distances" down the pores and consequent increased area accessible for charging of the electrode, the float-current exhibits larger initial values and shorter transition times, producing "high and narrow" i versus t float-current responses (Fig. 12c). In contrast, at lower H_2SO_4 concentrations, corresponding to less area of the electrode interface being "accessible", "low and broad" float-current shapes arise (Fig. 12a). Hence, float-current measurements can provide a direct and simple evaluation procedure for selecting optimal conditions for operating porous, high specific-area C-materials used for electrochemical capacitors. Experimental results from extended polarization ranges will provide additional evidence for this behaviour (see discussion in the next section).

3.4. Electrochemical damage to the C-cloth electrode under over-charge conditions

Increasing potential usually means an increase of state-of-charge of a capacitative electrode, including extension to over-charge conditions. In order to investigate such effects, a successive series of CVs of the C-cloth electrode, taken progressively in the positive-sweep direction beyond +0.8 V (RHE), were recorded as shown in Fig. 14. Extra accepted charge is obviously realized and, for $V < +1.1$ V, the extra anodic charge appears to be accumulated reversibly (see inset (a) of Fig. 14) indicating that the electrode can still keep good performance in an electrochemical capacitor device up to this potential limit. Note that, at higher potentials, the extra anodic charge is not, however, cathodically recovered until a potential range of ca. +0.6 to +0.2 V is reached in a reversed potential sweep, i.e. the recovery of charge has become irreversible. Such extra charge, therefore, is unavailable for capacitative charge and energy storage corresponding to the observable low coulombic and energy efficiencies of such charge/discharge processes.

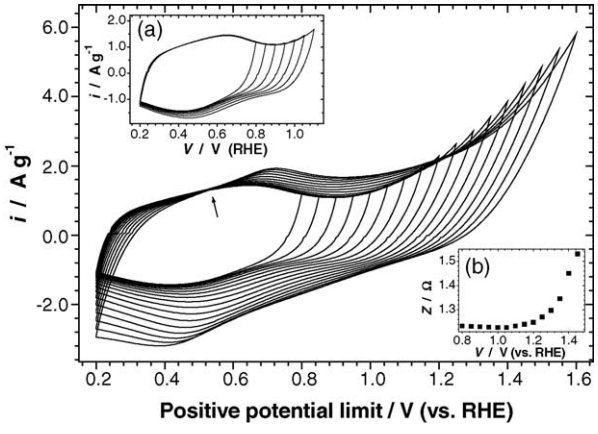

Fig. 14. A successive series of voltammograms, taken to progressively more positive potentials for a C-cloth electrode in 5 M H_2SO_4 at 5 mV s^{-1}. Inset (a) shows the voltammograms recorded below positive potential limit of +1.1 V and inset (b) shows how impedance, Z (=square-root of $[(Z')^2 + (Z'')^2]$), changes with polarization potentials from measurements at 10 Hz for every 50 mV between +0.8 and +1.35 V, RHE.

A common anodic current response is realized for electrodes cycled to a series of upper potential limits less than 1.2 V (see inset (a) in Fig. 14). However, for electrodes cycled positive to 1.2 V, the next anodic scan is no longer coincident with the previous scans. Also, a modified current peak at ca. $V = +0.7$ V becomes better defined as progressive scans are made up to more positive potentials. An isopotential point arises at $V = +0.52$ V as indicated by the arrow in Fig. 14, which suggests a transformation of species or functional groups at the C-cloth electrode, i.e. new surface functional groups are formed at the C-cloth electrode under over-charge conditions. Such new surface groups may arise either by oxidation of previously existing surface groups or by the breaking of outer C–C bonds of the C-structure producing new aldo or quinonoid groups which can be oxidized to carboxyl groups. No matter which processes are involved, the micro-chemical structure of the C-cloth is changed causing an increase of the impedance, Z, of the electrode as shown in the inset (b) of Fig. 14. Z begins to show significant increases at +1.1 V, which is the potential for onset of overcharge processes. Hence, this potential can be identified as a limit indicating the beginning of electrode damage if overcharge is made beyond that value.

In order further to investigate the possible damage of the C-cloth electrode under over-charge conditions, CV curves between potential limits of −0.05 to 1.1 V, RHE, at various scan rates were recorded, following polarization of the electrode at +1.6 V for 1 h. The results are shown in Fig. 15. Compared with Fig. 1, it is clear that the CV behaviour of the C electrode is totally changed after over-charge polarization. As a result of increased iR-drop, the CV curves show almost totally "resistive behaviour", even at 5 mV s^{-1}. Only by decreasing the scan rate to 1 mV s^{-1}, does the CV curve begin to regain some capacitative behaviour, especially on the cathodic scan for $V < +0.5$ V RHE (Fig. 15). In this case, the electrode exhibits only very small capacitative response or charge storage capacity on the anodic half-cycle between +0.6 and +1.1 V, showing high internal resistance and pore blockage characteristics. It may be expected that the over-charge oxidation also occurs at the internal micro-pores, which causes change in their interfaces or micro-porosity, and blocking of access of the electrolyte ions down into their double-layer interphases.

The float-current behaviour of the C-cloth electrode after over-charge polarization (Fig. 16) for 600 and 3600 s is com-

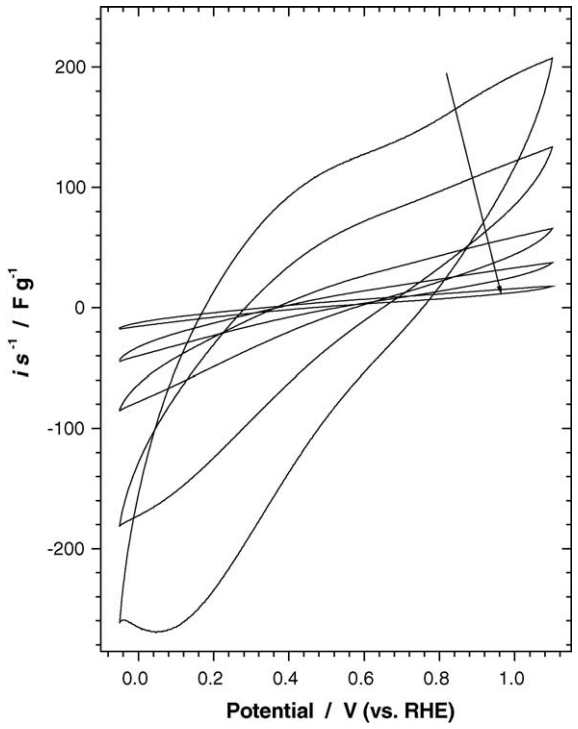

Fig. 15. Cyclic voltammograms of the C-cloth electrode in terms of capacitance response, i/s, in 5 M H_2SO_4 after polarizing at +1.6 V for 1 h for a sequential series of sweep-rates: 1, 2, 5, 10 and 25 mV s^{-1}. The arrow shows the direction of increasing sweep-rate.

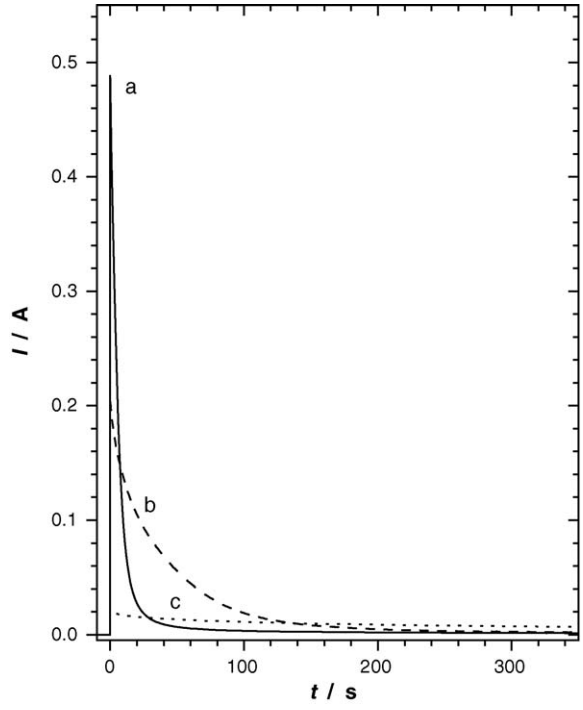

Fig. 16. Potentiostatic float-current responses recorded at the C-cloth electrode from polarization potential of +1.1 V for a duration 0 to 3600 s (figures show curves over a range from 0 to 300 s). Pretreatment of the C-cloth electrode: (a) fresh electrode; (b) after polarizing at +1.6 V for 600 s; (c) for 3600 s.

pared to that of a fresh electrode in Fig. 12. The initial float-current magnitudes after such polarizations (curves b and c in Fig. 16) decline appreciably down to as little as 5% of that without over-charge polarization (curve a in Fig. 16), and also the potentiostatic transition time becomes much longer, up to 3000 s, giving a very "low and broad" float-current profile. These are the characteristics of much lower "accessible area" of the electrode as discussed in Section 3.3.2, most probably due to the evidently unavoidable effect of blocking of nano- or micropores, with resulting increases of internal resistance, as indicated by the CV curves (Fig. 15).

3.5. Optimum potential window for operation of the C-cloth electrode

By analysis of the successive series of voltammograms shown in Fig. 14, a number of important quantitative parameters about the charge/discharge process of the C-cloth can be derived and are listed in Table 2. These parameters include the coulombic efficiency and the ratios of dQ/dV and $\Delta Q/\Delta V$. For a capacitative process the ratio dQ/dV is the differential capacitance (C_d) and $\Delta Q/\Delta V$ is the average capacitance (C_{ave}) for that process over the potential range ΔV. dQ/dV was evaluated on the positive potential sweep and $\Delta Q/\Delta V$

Table 2
Capacitance and coulombic efficiency values for various potential limits[a,b,c]

Positive potential limit (V)	+0.85	+0.95	+1.05	+1.15	+1.25	+1.35	+1.45	+1.55
Q (%)	99.5	99.0	97.8	95.2	89.8	83.1	74.9	65.9
dQ/dV (F g^{-1})	238	236	295	426	587	764	898	955
$\Delta Q/\Delta V$ (F g^{-1})	235	236	241	264	300	356	425	495
Negative potential limit (V)	−0.10	−0.20	−0.30	−0.40	−0.50	−0.60	−0.70	−0.80
Q (%)	100.5	99.9	97.5	94.3	91.0	86.7	83.0	76.8
dQ/dV (F g^{-1})	230	298	397	485	451	372	331	327
$\Delta Q/\Delta V$ (F g^{-1})	217	227	245	272	294	307	314	327

[a] Parameters were calculated based on a starting potential of +0.20 V for positive potential scans and +0.80 V for negative potential scans.
[b] dQ/dV and $\Delta Q/\Delta V$ (equivalent to differential capacitance, C_d, and average capacitance, C_{ave}, respectively, for potential < 1.0 V) were calculated from anodic charge in positive scans and from cathodic charge in negative scans.
[c] Error on Q: ±0.5; on $(\Delta Q/\Delta V)_d$ and $(\Delta Q/\Delta V)_{ave}$: ±1.

also calculated from the positive-going direction of potential change versus potential reversal limit.

The coulombic efficiency is maintained at almost 100% for $V <$ ca. +1.1 V (CV response is almost that of an ideal capacitor); beyond that potential, substantial decreases of coulombic and energy efficiency take place (at potential > +1.1 V the CV current response shows evidence of a Faradaic component).

Significantly, the good overall coulombic efficiency range (>95%) up to a potential of +1.15 V can be used as an indication of the positive practical potential limit for capacitative behaviour of the C-cloth electrode.

Over the potential range of +0.8 to +1.0 V (range of near ideal capacitative behaviour), C_d remains nearly constant at a value of 235 F g^{-1}. dQ/dV increases when $V > 1.0$ V and reaches 426 F g^{-1} at the positive potential limit of $V = +1.15$ V. However, when $V > 1.15$ V, though the ratio of dQ/dV still rises, no reversible chargeable capacitance is realized over this over-charge polarized region as mentioned above, rather the increased current is primarily the result of a Faradaic process. Furthermore, and significantly, the coulombic efficiency shows a rapid decrease from 95 to 67% in that region (Table 2).

Similar to the behaviour upon progressive scanning in the positive direction in Fig. 14, a successive series of voltammograms with potential-sweep extensions in the *negative direction*, were also examined for calculating dQ/dV and $\Delta Q/\Delta V$, as well as coulombic efficiency as a function of negative potential limit. The results are also listed in Table 2, which lists a negative potential limit for accepted reversible charging of the C-cloth electrode in H_2SO_4 as −0.4 V with ca. 95% coulombic efficiency. dQ/dV rises from 230 F g^{-1} in the potential range of +0.2 to −0.2 V up to 485 F g^{-1} at the above limit potential of −0.4 V. Again, as for scans in the positive direction, the extra charge passed beyond the reversible negative potential limit is only irreversibly accepted and thus cannot contribute to true capacitative charge and energy storage.

Note that the achieved capacitance value is dependent on the charge/discharge rate, as may be expected. Thus, at the low sweep-rate of 0.1 mV s^{-1} (ca. 0.36C rate), the capacitance can be expected to increase to more than 320–600 F g^{-1}.This is a conclusion of substantial practical significance.

4. Conclusions

The C-cloth electrode used in the present work shows excellent characteristics for construction of electrochemical capacitors. Almost reversible anodic and cathodic current responses are observed in a series of CVs (Fig. 1), corresponding to almost true capacitance behaviour. The electrode can be cycled with good coulombic efficiencies over the potential range of −0.4 to +1.15 V RHE with high capacitance of 230–485 F g^{-1} at an 18C rate, with good charge acceptance and delivery efficiency (>95%). Beyond that potential range, for both positive and negative potential directions, extra charge acceptance and delivery is observable, but is only achievable with substantial loss of coulombic efficiency coupled with electrochemical irreversibility, leading to poor energy efficiency in charge/discharge operations.

Because of the high specific-area and resultant fine porosity of the material studied in the present work, "charge or potential redistribution" and "penetration depth" effects dominate the processes of charging/discharging, and self-discharge, and affect float-current measurements. These effects are dependent on the pore resistance and are determined by both the charge/discharge rate and electrolyte concentration.

Self-discharge at the C-cloth electrode gives linear relationships between potential and logarithmic time (V versus log t). However, the rate, dV/d(log t), is not constant but depends on both the initial polarization potential and the charging current-density, an effect that is due to the porous nature of the C-cloth electrode and the consequent, time-dependent, charge redistribution down the pores. Charging at smaller current-densities leads to better signal "penetration depth" and a consequently more uniform charge distribution, i.e. between outer and inner layers of the C-cloth matrix, thus resulting initially in a smaller self-discharge rate. Conversely, at a larger current-density, charging takes place mainly at the outer regions of the electrode structure and can easily "flow out", corresponding initially to a larger self-discharge rate but usually from a smaller capacitance density.

The i–t curves obtained in the float-current measurements for the C-cloth electrode are different from those at traditional planar, bulk electrodes; potential transition-time scales at the former are much larger than at the latter. This is again due to the de Levie "porous electrode effect" [16] and the larger specific capacitance of the C-cloth electrode. Interestingly, in float-current measurements, the initial current magnitude and the transition time, corresponding to the shape of the current responses in relation to time, are found to be directly related to the pore resistance (electrolyte conductivity) and the "accessible area" of the C-cloth electrode. Increase in pore resistance and related decrease in "accessible area" causes the i–t responses to be changed from relatively "high and narrow" curves to ones of "low and broad" shape. The current responses in the float-current experiments can therefore be used as an indicator in the evaluation of carbon materials for double-layer capacitors, including identifying damage to electrode performance, e.g. after highly over-charge conditions.

Acknowledgement

Grateful acknowledgement is made to the Natural Sciences and Engineering Research Council of Canada for support of this work on a Strategic Research Grant (2003–2006).

References

[1] B.E. Conway, Electrochemical Supercapacitors: Scientific Principles and Technological Applications, Kluwer-Plenum, New York, 1999.
[2] J. Miller, in: S. Wolsky, N. Marincic (Eds.), Proceedings of the 2nd and 4th International Seminars on Electrochemical Capacitors and Similar Energy Storage Devices, Florida Educational Seminars, Boca Raton, FL, 1992 and 1994 (no pagination).
[3] B.E. Conway, in: S. Wolsky, N. Marincic (Eds.), Proceedings of the 7th International Symposium on Double-Layer Capacitors and Similar Energy Storage Devices, Florida Educational Seminars, Boca Raton, FL, 1997 (no pagination).
[4] C. Schmitt, H. Pröbstle, J. Fricke, J. Non-Crystalline Solids 285 (2001) 277.
[5] J. Niu, W.G. Pell, B.E. Conway, J. Power Sources 135 (2004) 332.
[6] A. Burke, in: S. Wolsky, N. Marincic (Eds.), Proceedings of the 4th International Seminar on Electrochemical Capacitors and Similar Energy Storage Devices, Florida Educational Seminars, Boca Raton, FL, 1993 and 1994 (no pagination).
[7] J. DeGaynor, R. Johnston, in: S. Wolsky, N. Marincic (Eds.), Proceedings of the 4th International Seminar on Electrochemical Capacitors and Similar Energy Storage Devices, Florida Educational Seminars, Boca Raton, FL, 1994 (no pagination).
[8] G. Pede, A. Iocabassi, S. Passerini, A. Bobbio, G. Botto, J. Power Sources 125 (2004) 280.
[9] A. Chu, P. Braatz, J. Power Sources 112 (2002) 236.
[10] B. Barnett, in: S. Wolsky, N. Marincic (Eds.), Proceedings of the 2nd International Seminar on Electrochemical Capacitors and Similar Energy Storage Devices, Florida Educational Seminars, Boca Raton, FL, 1992 (no pagination).
[11] S. Trasatti, G. Buzzanca, J. Appl. Electrochem. 4 (1974) 57.
[12] B.E. Conway, J. Motoza, Electrochim. Acta 28 (1983) 1;
B.E. Conway, J. Motoza, Electrochim. Acta 28 (1983) 57.
[13] R. Simpraga, J. Electroanal. Chem. 355 (1993) 79.
[14] G. Gryglewicz, J. Machnikowski, E. Lorenc-Grabowska, G. Lota, E. Trackowiak, Electrochim. Acta 50 (2005) 1197.
[15] B.E. Conway, W.G. Pell, T.-C. Liu, J. Power Sources 65 (1997) 53.
[16] R. de Levie, Electrochim. Acta 8 (1963) 751;
R. de Levie, Electrochim. Acta 9 (1964) 1231.
[17] E. Ayranci, B.E. Conway, Anal. Chem. 73 (2001) 1181.
[18] B.E. Conway, W.G. Pell, in: S. Wolsky, N. Marincic (Eds.), Proceedings of the 11th International Seminar on Electrochemical Capacitors and Similar Energy Storage Devices, Florida Educational Seminars, Boca Raton, FL, 2001 (no pagination).
[19] J. Ross Macdonald, Impedance Spectroscopy, John Wiley & Sons, NY, 1987.
[20] S. Hadzi-Jordanov, H. Angerstein-Kozlowska, B.E. Conway, J. Electroanal. Chem. 60 (1975) 359.
[21] B.E. Conway, W.G. Pell, J. Power Sources 105 (2002) 169.
[22] M.G. Sullivan, R. Kötz, O. Haas, J. Electrochem. Soc. 147 (2000) 308.
[23] D. Ragone, Proceedings of Society Automotive Engineers Conference, Detroit, MI, USA, May 1968.
[24] W.G. Pell, B.E. Conway, W.A. Adams, J. de Oliveira, J. Power Sources 80 (1999) 134.
[25] B.W. Ricketts, C. Ton That, J. Power Sources 89 (2001) 64.
[26] G. Gu, J. Kim, H. Song, G. Park, B. Park, Electrochim. Acta 45 (2000) 1533.
[27] N. Marincic, Kem. Ind. 54 (2005) 199.
[28] K. Kierzek, E. Frackowiak, G. Lota, G. Gryglewicz, J. Machnikowska, Electrochim. Acta 49 (2004) 515.
[29] P.D. Bennet, J.C. Currie, United States Patent 4,622,611, November 11, 1986.
[30] K. Kim, J. Hur, S. Jung, A. Kang, Electrochim. Acta 50 (2004) 863.
[31] M. Harada, T. Nishiyama, K. Toshihiko, K. Hiroyuki, S. Kaneko, M. Kurosaki, Y. Nakagawa, K. Mitani, T. Shinodo, Jpn. Kokai Tokkyo Koho (2003) 9 (JP2003107477).
[32] B.E. Conway, P.L. Bourgault, Trans. Faraday Soc. 58 (1962) 593.
[33] K. Kinoshta, Carbon, Wiley, New York, 1988.
[34] R.F. Strickland-Constable, Trans. Faraday Soc. 34 (1938) 1074.
[35] F.A. Posey, T. Morozumi, J. Electrochem. Soc. 113 (1966) 176.
[36] X. Jin, L. Zhuang, J. Lu, J. Electroanal. Chem. 519 (2001) 137.